Algebraic Bethe ansatz for the FPL^2 model

2004 J. Phys. A: Math. Gen. 37 7213

(http://iopscience.iop.org/0305-4470/37/29/004)

INSTITUTE OF PHYSICS PUBLISHING JOURNAL OF PHYSICS A: MATHEMATICAL AND GENERAL

J. Phys. A: Math. Gen. **37** (2004) 7213–7225 PII: S0305-4470(04)76762-1

Algebraic Bethe ansatz for the FPL^2 model

J Jacobsen and P Zinn-Justin

Laboratoire de Physique Théorique et Modèles Statistiques, Université Paris-Sud, Bâtiment 100, F-91405 Orsay Cedex, France

Received 18 February 2004, in final form 10 May 2004
Published 7 July 2004
Online at stacks.iop.org/JPhysA/37/7213
doi:10.1088/0305-4470/37/29/004

Abstract

An exact solution of the model of fully packed loops of two colours on a square lattice has recently been proposed by Dei Cont and Nienhuis using the coordinate Bethe ansatz approach. We point out here a simpler alternative, in which the transfer matrix is directly identified as a product of R-matrices; this allows us to apply the (nested) algebraic Bethe ansatz, which leads to the same Bethe equations. We comment on some of the applications of this result.

PACS numbers: 05.50.+q, 02.20.Uw, 02.30.Ik

(Some figures in this article are in colour only in the electronic version)

1. Introduction

Models of fluctuating loops play a key role in two-dimensional statistical physics, and a range of well-known models (Ising, Potts, percolation, O(n), to name but a few) can be conveniently studied through their reformulations as loop models. Exact results about loop models have been produced by a variety of techniques, including the Coulomb gas, conformal field theory, the Bethe ansatz and the stochastic Loewner evolution.

In this paper, we study the fully packed two-colour loop model on a square lattice (henceforth referred to as the FPL^2 model) from the point of view of the algebraic Bethe ansatz. The FPL^2 model was introduced in [1] as a generalization of the four-colouring model of the square lattice edges [2]. It is defined by assigning one of two colours (black or white) to each lattice edge, subject to the constraint that every vertex be incident to two black and two white edges. In this way, the black and white edges form fully packed loops which are given fugacities n_b and n_w depending on their colour.

The FPL^2 model has attracted much interest over the last decade. Successive advances in the Coulomb gas technique have permitted to compute the central charge and the critical exponents for a number of special cases: the four-colouring model $(n_b, n_w) = (2, 2)$ [2, 1], the dimer-loop model $(n_b, n_w) = (2, 1)$ [3] and the equal-fugacity case $n_b = n_w$ [4]. This

eventually led to the solution for general values of n_b and n_w [5]. An interesting special case is that of Hamiltonian walks, with $(n_b, n_w) = (0, 1)$ [6]. A generalization of the FPL^2 model, obtained by giving the loops a bending rigidity, was given in [7]. It contains as a special case the so-called Flory model of protein melting [8].

All these Coulomb gas results are obtained by making certain reasonable, but non-rigorous, assumptions about the long wavelength behaviour of an associated interface model. The resulting critical exponents are however believed to be exact, and they have been successfully tested against numerical Monte Carlo [1, 3] and transfer matrix [9, 6, 7] results.

To give the results obtained by the Coulomb gas a rigorous status, and to go beyond it and derive results which are not obtainable from a continuum approach, it is natural to turn to the methods of integrability. Following earlier work on the four-colouring model [10], Dei Cont and Nienhuis [11] have very recently succeeded in finding a coordinate Bethe ansatz for the equal-fugacity FPL^2 model. In particular, they have computed the exact free energy in the thermodynamic limit. Moreover, they have shown that when $n_b \neq n_w$, the FPL^2 model is not integrable, in agreement with earlier expectations [6].

However, the coordinate Bethe ansatz is a rather complex technique, which, in order to be made fully rigorous, would require investigation of a large number of specific configurations. The goal of the present paper is to present a simpler alternative, in which the transfer matrix of the equal-fugacity FPL^2 model (henceforth we note $n \equiv n_b = n_w$) is identified with a product of trigonometric R-matrices of $U_q(\widehat{sl(4)})$ with $n = -q - q^{-1}$ (and an appropriate twist). Applying the (nested) algebraic Bethe ansatz allows us to recover the Bethe equations of [11] in a straigthforward fashion. As a bonus we obtain the central charge and the critical exponents, which are found to agree with the non-rigorous results of [6]. We also comment on an $n \to -n$ symmetry of some of the sectors of the transfer matrix.

The paper is organized as follows. The FPL^2 model is defined in section 2. In section 3 we define its transfer matrix in terms of an R-matrix that adds four vertices and a twist matrix that takes care of the boundary conditions. We then show how these matrices are related to those of the affine quantum group $U_q(\widehat{sl(4)})$ with alternating fundamental and conjugate representations. The corresponding Bethe ansatz equations are discussed in section 4, and we reproduce, in particular, the eigenvalues of the transfer matrix [11]. Finally, in section 5, we give the expressions of the central charge and conformal weights for $n \leqslant 2$, and we compare our results to those obtained for fully packed loops on the hexagonal lattice.

2. The FPL^2 model

Following [6], we reformulate the FPL^2 model as a 24-vertex model. For each vertex of the square lattice, the four incident edges are decorated with arrows of two possible orientations (outgoing or ingoing with respect to the vertex) and two possible colours (black or white), subject to the constraint that each of the four possibilities be represented exactly once around every vertex. Clearly, following the arrows of a given colour traces out an oriented loop of that colour. Note that reversing the arrows along any one loop, and leaving all other arrows unchanged, leads to another allowed configuration.

We then assign a weight $w = w_b w_w$ to each vertex which is the product of weights w_b and w_w coming from the oriented black and white loops, respectively. The black weight $w_b = \omega$ (resp. $w_b = \omega^{-1}$) when the black loop makes a right turn (resp. a left turn) at the concerned vertex and $w_b = 1$ when the black loop goes straight. For the white weight we choose the opposite convention, that is, with ω and ω^{-1} exchanged. The weights of the six types of vertices which are unrelated by $\pi/2$ rotations are given in figure 1.

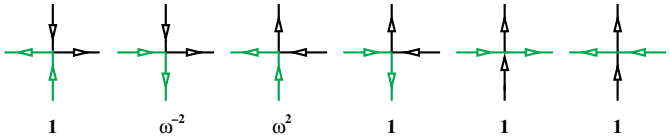

Figure 1. The six types of vertices in the 24-vertex model (the remaining vertices are obtained by $\pi/2$ rotations) with their corresponding weights.

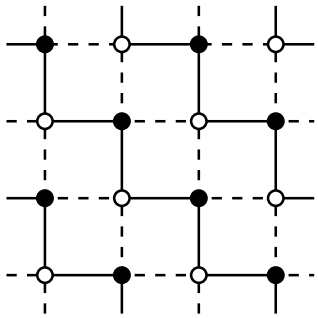

Figure 2. Parity convention for vertices and edges of the square lattice. Even (resp. odd) edges are shown in dashed (resp. solid) lines. Even (resp. odd) vertices are shown as open (resp. solid) circles.

The FPL^2 model with fugacity n for both colours of loops is recovered by summing independently over the orientations of all loops (black and white). An anticlockwise (resp. clockwise) black loop contributes ω^4 (resp. ω^{-4}) to the fugacity, as it must turn four times more (resp. less) to the left than to the right. Thus, ω is fixed by

$$n = \omega^4 + \omega^{-4}. \tag{2.1}$$

In order to apply the Bethe ansatz it is important to specify the boundary conditions. In the following we shall specialize to the case where the square lattice is wrapped on a cylinder, i.e., with periodic boundary conditions across a horizontal row of $2L$ vertices [6, 11]. Note that the argument leading to (2.1) only works for contractible loops, i.e., loops that do not wrap around the periodic direction. To obtain the correct weight also for non-contractible loops, one introduces a vertical seam separating the first and the last vertex in each row [11]. Horizontal edges cutting the seam are assigned an extra weight of a (resp. a^{-1}) when covered by a left-pointing (resp. right-pointing) arrow; the convention does *not* depend on the colour of the arrow. Clearly, non-contractible loops can only wind once, so a is fixed by

$$n = a + a^{-1}. \tag{2.2}$$

With these boundary conditions, the FPL^2 model contains three conserved quantities [11]. To explain these, we shall adopt a convention for the parity of both the vertices and the edges, as shown in figure 2. The three components of the conserved charge which are conserved by the evolution along the cylinder are

$$Q = \begin{pmatrix} L \\ L \\ L \end{pmatrix} - \begin{pmatrix} N_{w\downarrow} + N_{eb} \\ N_{\downarrow} \\ N_{w\downarrow} + N_{ob} \end{pmatrix} \tag{2.3}$$

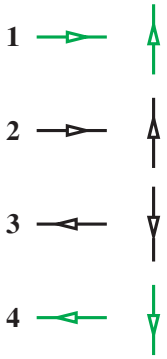

Figure 3. Convention for the labelling of arrow states on an even edge.

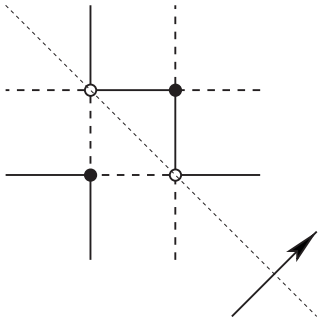

Figure 4. The FPL^2 model R-matrix adds two even and two odd vertices as shown. The arrow indicates the transfer direction. The parity of vertices and edges follows the conventions of figure 2. The four dangling edges below (resp. above) the thin dashed line specify the in-state (resp. the out-state).

where N is the number of vertical edges of a given parity ($e =$ even, $o =$ odd) in the concerned row, b (black) or w (white) refers to the colour of the arrow and $\uparrow$ (up) or $\downarrow$ (down) to its orientation. The constant term has been added for convenience. Strictly speaking, it would make better sense to talk about conserved charges with respect to a parity convention for the columns that does not alternate from row to row. In this respect, the charges (2.3) only commute with the transfer matrix that adds *two rows* at a time.

3. The transfer matrix

Before proceeding further we shall adopt a convention for labelling the arrow state $i = 1, 2, 3, 4$ of each edge in the FPL^2 model. This is shown in figure 3 for the case of an even edge; the convention for an odd edge is similar, but with all arrows reversed (i.e., $i \to 5 - i$).

We have seen above that from the point of view of the conserved charges, it is most natural to build up the lattice by adding two rows at a time. We have also assumed that the horizontal strip is of even width $2L$. In order to define the row-to-row transfer matrix T, we first define a 256×256 matrix, which we denote, in analogy with integrable models, by R; it adds four vertices as shown in figure 4. Using the weights of figure 1, it is straightforward to write R

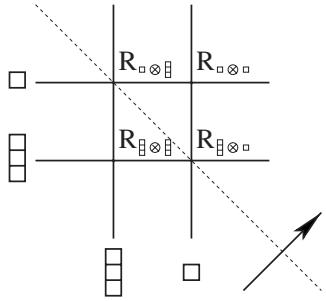

Figure 5. R-matrix for two rows and two columns, which alternatingly carry the fundamental representation of $U_q(\widehat{sl(4)})$ and its conjugate. The arrow indicates the transfer direction.

explicitly, in the basis obtained by using the labelling of figure 3 for the external lines and by taking the tensor product of the corresponding vector spaces.

The transfer matrix that propagates the system in the upwards direction then reads

$$T = \mathrm{tr}_a\, R_{aL} \cdots R_{a2} R_{a1} (\Omega^{-1} \otimes \Omega) \tag{3.1}$$

where the subscript a denotes the 'auxiliary space' (the pair of horizontal lines) of dimension 16 and the subscripts $1, 2, \ldots, L$ correspond to the L pairs of vertical lines which form the 'physical space'. The twist $\Omega^{-1} \otimes \Omega$ is a matrix in the auxiliary space which takes care of the effect of the seam; explicitly, $\Omega = \mathrm{diag}(1/a, 1/a, a, a)$ acts on the upper horizontal line whereas Ω^{-1} acts on the lower line. Note that this form of the twist has previously been considered in [12, 13].

We now introduce another R-matrix which is related to the affine quantum group $U_q(\widehat{sl(4)})$, where $q = -\omega^{-4}$ (so that $n = -q - q^{-1}$), and which we call $\mathbf{R}$. It is schematically described figure 5, in which the two representations $\square$ and $\begin{smallmatrix}\square\\\square\end{smallmatrix}$ of $U_q(\widehat{sl(4)})$ appear in an alternating fashion. Conventions are such that at a vertex where two lines intersect, the first factor in the tensor product refers to the leftmost line of the in-state, when seen along the transfer direction.

The four R-matrices which appear in figure 5 can be expressed as [14]

$$\check{\mathbf{R}}_{\square\otimes\square}(x) = (qx - q^{-1}x^{-1})\check{\mathbf{P}}^{\square\square}_{\square\otimes\square} + (qx^{-1} - q^{-1}x)\check{\mathbf{P}}^{\begin{smallmatrix}\square\\\square\end{smallmatrix}}_{\square\otimes\square} \tag{3.2a}$$

$$\check{\mathbf{R}}_{\square\otimes\begin{smallmatrix}\square\\\square\end{smallmatrix}}(x) = (q^2x - q^{-2}x^{-1})\check{\mathbf{P}}^{\begin{smallmatrix}\square\square\\\square\end{smallmatrix}}_{\square\otimes\begin{smallmatrix}\square\\\square\end{smallmatrix}} + (q^2x^{-1} - q^{-2}x)\check{\mathbf{P}}^{\emptyset}_{\square\otimes\begin{smallmatrix}\square\\\square\end{smallmatrix}} \tag{3.2b}$$

$$\check{\mathbf{R}}_{\begin{smallmatrix}\square\\\square\end{smallmatrix}\otimes\square}(x) = (q^2x - q^{-2}x^{-1})\check{\mathbf{P}}^{\begin{smallmatrix}\square\square\\\square\end{smallmatrix}}_{\begin{smallmatrix}\square\\\square\end{smallmatrix}\otimes\square} + (q^2x^{-1} - q^{-2}x)\check{\mathbf{P}}^{\emptyset}_{\begin{smallmatrix}\square\\\square\end{smallmatrix}\otimes\square} \tag{3.2c}$$

$$\check{\mathbf{R}}_{\begin{smallmatrix}\square\\\square\end{smallmatrix}\otimes\begin{smallmatrix}\square\\\square\end{smallmatrix}}(x) = (qx - q^{-1}x^{-1})\check{\mathbf{P}}^{\begin{smallmatrix}\square\square\\\square\square\end{smallmatrix}}_{\begin{smallmatrix}\square\\\square\end{smallmatrix}\otimes\begin{smallmatrix}\square\\\square\end{smallmatrix}} + (qx^{-1} - q^{-1}x)\check{\mathbf{P}}^{\begin{smallmatrix}\square\\\square\end{smallmatrix}}_{\begin{smallmatrix}\square\\\square\end{smallmatrix}\otimes\begin{smallmatrix}\square\\\square\end{smallmatrix}}. \tag{3.2d}$$

We have, as usual, denoted $\check{\mathbf{R}} \equiv \Pi\mathbf{R}$, where Π is the operator that permutes the two factors of the tensor product. The $\check{\mathbf{P}}$ are intertwining operators of $U_q(sl(4))$ which can be computed using representation theory; the parameter x is the ratio of spectral parameters of the horizontal and vertical lines. We shall give the explicit matrix representations of the R-matrices below, after fixing the values of x.

In the present context, one can first define separately transfer matrices for even and odd rows (however, only their product will be directly related to the previous transfer matrix T). Indeed, we define $\mathbf{R}_{\begin{smallmatrix}\square\\\square\end{smallmatrix}}(x) = \mathbf{R}_{\begin{smallmatrix}\square\\\square\end{smallmatrix}\otimes\square}(x/x_\square)\mathbf{R}_{\begin{smallmatrix}\square\\\square\end{smallmatrix}\otimes\begin{smallmatrix}\square\\\square\end{smallmatrix}}(x/x_{\begin{smallmatrix}\square\\\square\end{smallmatrix}})$ and $\mathbf{R}_\square(x) = \mathbf{R}_{\square\otimes\square}(x/x_\square)\mathbf{R}_{\square\otimes\begin{smallmatrix}\square\\\square\end{smallmatrix}}(x/x_{\begin{smallmatrix}\square\\\square\end{smallmatrix}})$, where the products are meant as in figure 5, and the spectral parameters of vertical lines $x_{\begin{smallmatrix}\square\\\square\end{smallmatrix}}$, $x_\square$ are supposed to be fixed. Next define

$$\mathbf{T}_{\begin{smallmatrix}\square\\\square\end{smallmatrix}}(x) = \mathrm{tr}_{\begin{smallmatrix}\square\\\square\end{smallmatrix}}\mathbf{R}_{\begin{smallmatrix}\square\\\square\end{smallmatrix}L}(x)\cdots\mathbf{R}_{\begin{smallmatrix}\square\\\square\end{smallmatrix}2}(x)\mathbf{R}_{\begin{smallmatrix}\square\\\square\end{smallmatrix}1}(x)\Omega^{-1} \tag{3.3a}$$

$$\mathbf{T}_\square(x) = \mathrm{tr}_\square\mathbf{R}_{\square L}(x)\cdots\mathbf{R}_{\square 2}(x)\mathbf{R}_{\square 1}(x)\Omega \tag{3.3b}$$

where, as before, the indices determine the spaces on which the matrices act. Note that Ω and Ω^{-1} can be considered as the same element of the Cartan subalgebra of $U_q(\widehat{sl(4)})$, but in fundamental and conjugate representations, respectively. Due to the Yang–Baxter equation, the $\mathbf{T}_{\begin{smallmatrix}\square\\\square\end{smallmatrix}}(x)$ and $\mathbf{T}_\square(x)$ form an infinite family of commuting matrices; their product, the two-row transfer matrix $\mathbf{T}(x, y) = \mathbf{T}_\square(x)\mathbf{T}_{\begin{smallmatrix}\square\\\square\end{smallmatrix}}(y) = \mathbf{T}_{\begin{smallmatrix}\square\\\square\end{smallmatrix}}(y)\mathbf{T}_\square(x)$, is itself of the form

$$\mathbf{T}(x, y) = \mathrm{tr}_a\mathbf{R}_{aL}(x, y)\cdots\mathbf{R}_{a2}(x, y)\mathbf{R}_{a1}(x, y)(\Omega^{-1}\otimes\Omega) \tag{3.4}$$

where $\mathbf{R}(x, y) = \mathbf{R}_\square(x)\mathbf{R}_{\begin{smallmatrix}\square\\\square\end{smallmatrix}}(y)$.

We now claim that the two R-matrices for two rows and two columns R and $\mathbf{R}$, which we have introduced, are relate. At this point we choose all horizontal lines (whether odd or even) to have the same spectral parameter, and similarly for all vertical lines, so that the ratio is constant and is $x = q^{-1}$. Note that at this unique value, the matrices $\check{\mathbf{R}}_{\square\otimes\square}$ and $\check{\mathbf{R}}_{\begin{smallmatrix}\square\\\square\end{smallmatrix}\otimes\begin{smallmatrix}\square\\\square\end{smallmatrix}}$ become proportional to projectors onto the antisymmetric sub-representations. This enforces the fact that at each vertex the four arrow states in figure 3 are each represented exactly once, i.e., among the 256 possible vertex states only the 24 shown in figure 1 will carry nonzero weight.

Explicitly ($c = q^{-1} - q$)

$\check{\mathbf{R}}_{\square\otimes\square}(q)$

$$= c\begin{pmatrix}
0 & 0 & 0 & 0 & 0 & 0 & 0 & 0 & 0 & 0 & 0 & 0 & 0 & 0 & 0 & 0\\
0 & -q & 0 & 0 & 1 & 0 & 0 & 0 & 0 & 0 & 0 & 0 & 0 & 0 & 0 & 0\\
0 & 0 & -q & 0 & 0 & 0 & 0 & 0 & 1 & 0 & 0 & 0 & 0 & 0 & 0 & 0\\
0 & 0 & 0 & -q & 0 & 0 & 0 & 0 & 0 & 0 & 0 & 0 & 1 & 0 & 0 & 0\\
0 & 1 & 0 & 0 & -q^{-1} & 0 & 0 & 0 & 0 & 0 & 0 & 0 & 0 & 0 & 0 & 0\\
0 & 0 & 0 & 0 & 0 & 0 & 0 & 0 & 0 & 0 & 0 & 0 & 0 & 0 & 0 & 0\\
0 & 0 & 0 & 0 & 0 & 0 & -q & 0 & 0 & 1 & 0 & 0 & 0 & 0 & 0 & 0\\
0 & 0 & 0 & 0 & 0 & 0 & 0 & -q & 0 & 0 & 0 & 0 & 0 & 1 & 0 & 0\\
0 & 0 & 1 & 0 & 0 & 0 & 0 & 0 & -q^{-1} & 0 & 0 & 0 & 0 & 0 & 0 & 0\\
0 & 0 & 0 & 0 & 0 & 0 & 1 & 0 & 0 & -q^{-1} & 0 & 0 & 0 & 0 & 0 & 0\\
0 & 0 & 0 & 0 & 0 & 0 & 0 & 0 & 0 & 0 & 0 & 0 & 0 & 0 & 0 & 0\\
0 & 0 & 0 & 0 & 0 & 0 & 0 & 0 & 0 & 0 & 0 & -q & 0 & 0 & 1 & 0\\
0 & 0 & 0 & 1 & 0 & 0 & 0 & 0 & 0 & 0 & 0 & 0 & -q^{-1} & 0 & 0 & 0\\
0 & 0 & 0 & 0 & 0 & 0 & 0 & 1 & 0 & 0 & 0 & 0 & 0 & -q^{-1} & 0 & 0\\
0 & 0 & 0 & 0 & 0 & 0 & 0 & 0 & 0 & 0 & 0 & 1 & 0 & 0 & -q^{-1} & 0\\
0 & 0 & 0 & 0 & 0 & 0 & 0 & 0 & 0 & 0 & 0 & 0 & 0 & 0 & 0 & 0
\end{pmatrix} \tag{3.5a}$$

$$\check{\mathbf{R}}_{\square\otimes\begin{smallmatrix}\square\\\square\end{smallmatrix}}(q) = c\begin{pmatrix}
0 & 0 & 0 & 0 & 0 & -q & 0 & 0 & 0 & 0 & -q^3 & 0 & 0 & 0 & 0 & -q^5 \\
0 & 0 & 0 & 0 & 1 & 0 & 0 & 0 & 0 & 0 & 0 & 0 & 0 & 0 & 0 & 0 \\
0 & 0 & 0 & 0 & 0 & 0 & 0 & 0 & 1 & 0 & 0 & 0 & 0 & 0 & 0 & 0 \\
0 & 0 & 0 & 0 & 0 & 0 & 0 & 0 & 0 & 0 & 0 & 0 & 1 & 0 & 0 & 0 \\
0 & 1 & 0 & 0 & 0 & 0 & 0 & 0 & 0 & 0 & 0 & 0 & 0 & 0 & 0 & 0 \\
-q^{-1} & 0 & 0 & 0 & 0 & 0 & 0 & 0 & 0 & 0 & -q & 0 & 0 & 0 & 0 & -q^3 \\
0 & 0 & 0 & 0 & 0 & 0 & 0 & 0 & 0 & 1 & 0 & 0 & 0 & 0 & 0 & 0 \\
0 & 0 & 0 & 0 & 0 & 0 & 0 & 0 & 0 & 0 & 0 & 0 & 0 & 1 & 0 & 0 \\
0 & 0 & 1 & 0 & 0 & 0 & 0 & 0 & 0 & 0 & 0 & 0 & 0 & 0 & 0 & 0 \\
0 & 0 & 0 & 0 & 0 & 0 & 1 & 0 & 0 & 0 & 0 & 0 & 0 & 0 & 0 & 0 \\
-q^{-3} & 0 & 0 & 0 & 0 & -q^{-1} & 0 & 0 & 0 & 0 & 0 & 0 & 0 & 0 & 0 & -q \\
0 & 0 & 0 & 0 & 0 & 0 & 0 & 0 & 0 & 0 & 0 & 0 & 0 & 0 & 1 & 0 \\
0 & 0 & 0 & 1 & 0 & 0 & 0 & 0 & 0 & 0 & 0 & 0 & 0 & 0 & 0 & 0 \\
0 & 0 & 0 & 0 & 0 & 0 & 0 & 1 & 0 & 0 & 0 & 0 & 0 & 0 & 0 & 0 \\
0 & 0 & 0 & 0 & 0 & 0 & 0 & 0 & 0 & 0 & 0 & 1 & 0 & 0 & 0 & 0 \\
-q^{-5} & 0 & 0 & 0 & 0 & -q^{-3} & 0 & 0 & 0 & 0 & -q^{-1} & 0 & 0 & 0 & 0 & 0
\end{pmatrix} \tag{3.5b}$$

$$\check{\mathbf{R}}_{\begin{smallmatrix}\square\\\square\end{smallmatrix}\otimes\square}(q) = c\begin{pmatrix}
0 & 0 & 0 & 0 & 0 & -q & 0 & 0 & 0 & 0 & -q & 0 & 0 & 0 & 0 & -q \\
0 & 0 & 0 & 0 & 1 & 0 & 0 & 0 & 0 & 0 & 0 & 0 & 0 & 0 & 0 & 0 \\
0 & 0 & 0 & 0 & 0 & 0 & 0 & 0 & 1 & 0 & 0 & 0 & 0 & 0 & 0 & 0 \\
0 & 0 & 0 & 0 & 0 & 0 & 0 & 0 & 0 & 0 & 0 & 0 & 1 & 0 & 0 & 0 \\
0 & 1 & 0 & 0 & 0 & 0 & 0 & 0 & 0 & 0 & 0 & 0 & 0 & 0 & 0 & 0 \\
-q^{-1} & 0 & 0 & 0 & 0 & 0 & 0 & 0 & 0 & 0 & -q & 0 & 0 & 0 & 0 & -q \\
0 & 0 & 0 & 0 & 0 & 0 & 0 & 0 & 0 & 1 & 0 & 0 & 0 & 0 & 0 & 0 \\
0 & 0 & 0 & 0 & 0 & 0 & 0 & 0 & 0 & 0 & 0 & 0 & 0 & 1 & 0 & 0 \\
0 & 0 & 1 & 0 & 0 & 0 & 0 & 0 & 0 & 0 & 0 & 0 & 0 & 0 & 0 & 0 \\
0 & 0 & 0 & 0 & 0 & 0 & 1 & 0 & 0 & 0 & 0 & 0 & 0 & 0 & 0 & 0 \\
-q^{-1} & 0 & 0 & 0 & 0 & -q^{-1} & 0 & 0 & 0 & 0 & 0 & 0 & 0 & 0 & 0 & -q \\
0 & 0 & 0 & 0 & 0 & 0 & 0 & 0 & 0 & 0 & 0 & 0 & 0 & 0 & 1 & 0 \\
0 & 0 & 0 & 1 & 0 & 0 & 0 & 0 & 0 & 0 & 0 & 0 & 0 & 0 & 0 & 0 \\
0 & 0 & 0 & 0 & 0 & 0 & 0 & 1 & 0 & 0 & 0 & 0 & 0 & 0 & 0 & 0 \\
0 & 0 & 0 & 0 & 0 & 0 & 0 & 0 & 0 & 0 & 0 & 1 & 0 & 0 & 0 & 0 \\
-q^{-1} & 0 & 0 & 0 & 0 & -q^{-1} & 0 & 0 & 0 & 0 & -q^{-1} & 0 & 0 & 0 & 0 & 0
\end{pmatrix} \tag{3.5c}$$

$$\check{\mathbf{R}}_{\begin{smallmatrix}\square&\square\\\square&\square\end{smallmatrix}}(q) = c\begin{pmatrix}
0 & 0 & 0 & 0 & 0 & 0 & 0 & 0 & 0 & 0 & 0 & 0 & 0 & 0 & 0 & 0 \\
0 & -q^{-1} & 0 & 0 & 1 & 0 & 0 & 0 & 0 & 0 & 0 & 0 & 0 & 0 & 0 & 0 \\
0 & 0 & -q^{-1} & 0 & 0 & 0 & 0 & 0 & 1 & 0 & 0 & 0 & 0 & 0 & 0 & 0 \\
0 & 0 & 0 & -q^{-1} & 0 & 0 & 0 & 0 & 0 & 0 & 0 & 0 & 1 & 0 & 0 & 0 \\
0 & 1 & 0 & 0 & -q & 0 & 0 & 0 & 0 & 0 & 0 & 0 & 0 & 0 & 0 & 0 \\
0 & 0 & 0 & 0 & 0 & 0 & 0 & 0 & 0 & 0 & 0 & 0 & 0 & 0 & 0 & 0 \\
0 & 0 & 0 & 0 & 0 & 0 & -q^{-1} & 0 & 0 & 1 & 0 & 0 & 0 & 0 & 0 & 0 \\
0 & 0 & 0 & 0 & 0 & 0 & 0 & -q^{-1} & 0 & 0 & 0 & 0 & 0 & 1 & 0 & 0 \\
0 & 0 & 1 & 0 & 0 & 0 & 0 & 0 & -q & 0 & 0 & 0 & 0 & 0 & 0 & 0 \\
0 & 0 & 0 & 0 & 0 & 0 & 1 & 0 & 0 & -q & 0 & 0 & 0 & 0 & 0 & 0 \\
0 & 0 & 0 & 0 & 0 & 0 & 0 & 0 & 0 & 0 & 0 & 0 & 0 & 0 & 0 & 0 \\
0 & 0 & 0 & 0 & 0 & 0 & 0 & 0 & 0 & 0 & 0 & -q^{-1} & 0 & 0 & 1 & 0 \\
0 & 0 & 0 & 1 & 0 & 0 & 0 & 0 & 0 & 0 & 0 & 0 & -q & 0 & 0 & 0 \\
0 & 0 & 0 & 0 & 0 & 0 & 0 & 1 & 0 & 0 & 0 & 0 & 0 & -q & 0 & 0 \\
0 & 0 & 0 & 0 & 0 & 0 & 0 & 0 & 0 & 0 & 0 & 1 & 0 & 0 & -q & 0 \\
0 & 0 & 0 & 0 & 0 & 0 & 0 & 0 & 0 & 0 & 0 & 0 & 0 & 0 & 0 & 0
\end{pmatrix}. \tag{3.5d}$$

Note that we use the standard bases for $\square$ and $\begin{smallmatrix}\square\\\square\end{smallmatrix}$ (which are dual bases of each other).

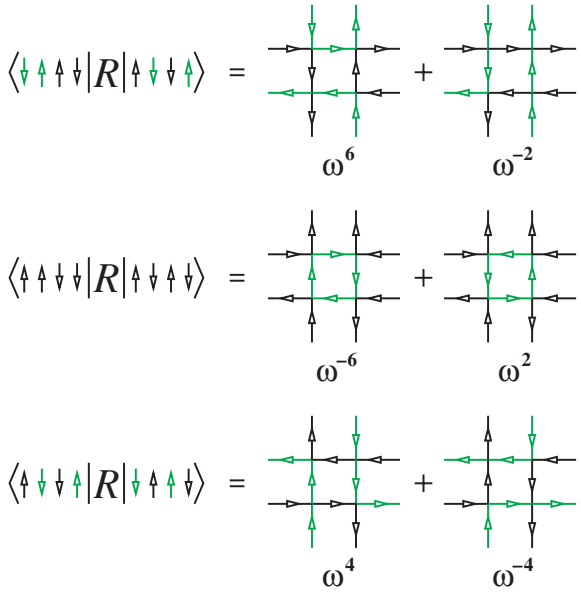

Figure 6. Examples of non-trivial R-matrix elements in the FPL^2 model.

One can then check that

$$\mathbf{R} = c^4 U R U^{-1} \tag{3.6}$$

where the constant c^4 takes care of the extra factors in equations (3.5) and U is a diagonal matrix that fully factorizes as a tensor product over the four incoming lines: $U = U_{h\square} \otimes U_{h\begin{smallmatrix}\square\\\square\end{smallmatrix}} \otimes U_{v\begin{smallmatrix}\square\\\square\end{smallmatrix}} \otimes U_{v\square}$, with as a possible choice

$$\begin{aligned} U_{h\square} &= \begin{pmatrix} \omega^6 & 0 & 0 & 0 \\ 0 & \omega^4 & 0 & \\ 0 & 0 & \omega^2 & 0 \\ 0 & 0 & 0 & 1 \end{pmatrix} & U_{h\begin{smallmatrix}\square\\\square\end{smallmatrix}} &= \begin{pmatrix} \omega^6 & 0 & 0 & 0 \\ 0 & \omega^4 & 0 & 0 \\ 0 & 0 & \omega^2 & 0 \\ 0 & 0 & 0 & 1 \end{pmatrix} \\ U_{v\square} &= \begin{pmatrix} \omega^{12} & 0 & 0 & 0 \\ 0 & \omega^8 & 0 & 0 \\ 0 & 0 & \omega^4 & 0 \\ 0 & 0 & 0 & 1 \end{pmatrix} & U_{v\begin{smallmatrix}\square\\\square\end{smallmatrix}} &= \begin{pmatrix} \omega^{-6} & 0 & 0 & 0 \\ 0 & \omega^{-4} & 0 & 0 \\ 0 & 0 & \omega^{-2} & 0 \\ 0 & 0 & 0 & 1 \end{pmatrix}. \end{aligned} \tag{3.7}$$

Consequently, the corresponding transfer matrices T and $\mathbf{T}$ are also similar up to a constant:

$$\mathbf{T} = c^{4L} U_v T U_v^{-1} \tag{3.8}$$

where U_v is the tensor product of $U_{v\begin{smallmatrix}\square\\\square\end{smallmatrix}}$ and $U_{v\square}$ for all vertical lines.

Obviously, space does not permit us to reproduce the resulting 256×256 matrices R and $\mathbf{R}$. Rather, figure 6 gives three examples of matrix elements. Note that our convention for the R-matrix (see figure 4) is to keep fixed indices for the horizontal and vertical lines. Thus, if the arrow configuration (coded as in figure 1) is $\rho_4\rho_3\rho_2\rho_1$ for the out-state (read from left to right when looking along the transfer direction), it is $\rho_2\rho_1\rho_4\rho_3$ for the in-state. The three examples in figure 6 then read explicitly $R_{81,18} = \omega^6 + \omega^{-2}$; $R_{103,91} = \omega^{-6} + \omega^2$ and $R_{239,188} = \omega^4 + \omega^{-4}$. The corresponding entries of $\mathbf{R}$ are found from (3.6).

4. Algebraic Bethe ansatz

The set of commuting transfer matrices $\mathbf{T}_{\square}(x)$, $\mathbf{T}_{\begin{smallmatrix}\square\\\square\end{smallmatrix}}(x)$ can be diagonalized using the so-called nested Bethe ansatz. We shall not describe this procedure here and refer to [15–17] for details. The eigenstates are built by the action of operators which depend on parameters that we call $u_k^{(i)}$, with $i = 1, 2, 3$ and $k = 1, \ldots, m^{(i)}$, on a reference eigenstate (highest weight state) which has only white arrows pointing up. These parameters satisfy equations, which, in our parametrization, are algebraic in the $\mathrm{e}^{\mathrm{i}\gamma u_k^{(i)}}$, where γ is such that $q = -\mathrm{e}^{-\mathrm{i}\gamma}$. Explicitly, call $\omega^{(i)}$ the diagonal elements of the twist Ω in the fundamental representation (here, $\omega^{(1)} = \omega^{(2)} = 1/a, \omega^{(3)} = \omega^{(4)} = a$), with $\prod_{i=1}^{4} \omega^{(i)} = 1$; and define the functions $Q^{(i)}(u) = \prod_{k=1}^{m^{(i)}} \sin\gamma\big(u - u_k^{(i)}\big)$, $i = 1, 2, 3$. $Q^{(0)} \equiv Q^{(4)} \equiv 1$. Then the Bethe ansatz equations read

$$-\frac{Q^{(i+1)}\big(u_k^{(i)}+1\big)}{Q^{(i+1)}\big(u_k^{(i)}\big)}\,\frac{Q^{(i)}\big(u_k^{(i)}-1\big)}{Q^{(i)}\big(u_k^{(i)}+1\big)}\,\frac{Q^{(i-1)}\big(u_k^{(i)}\big)}{Q^{(i-1)}\big(u_k^{(i)}-1\big)} = \frac{\omega^{(i)}}{\omega^{(i+1)}}\,\frac{f^{(i)}\big(u_k^{(i)}\big)}{f^{(i+1)}\big(u_k^{(i)}\big)} \tag{4.1}$$

for $1 \leqslant i \leqslant 3, 1 \leqslant k \leqslant m^{(i)}$. The functions $f^{(i)}$ depend on the representations and spectral parameters of the physical space (and on the twist); here, one easily computes $f^{(1)}(u) = \omega^{(1)}(\sin\gamma u \sin\gamma(u-1))^L$, $f^{(i)}(u) = \omega^{(i)}(\sin\gamma(u+1)\sin\gamma(u-1))^L$ for $i = 2, 3$, $f^{(4)}(u) = \omega^{(4)}(\sin\gamma(u+1)\sin\gamma u)^L$.

The corresponding eigenvalues of $\mathbf{T}_{\begin{smallmatrix}\square\\\square\end{smallmatrix}}(u)$ and $\mathbf{T}_{\square}(u)$, in the parametrization $x = -\mathrm{e}^{\mathrm{i}\gamma(u+1)}$, are

$$t_{\square}(u) = X^{(1)}(u) + X^{(2)}(u) + X^{(3)}(u) + X^{(4)}(u) \tag{4.2a}$$

$$t_{\begin{smallmatrix}\square\\\square\end{smallmatrix}}(u) = \tilde{X}^{(1)}(u) + \tilde{X}^{(2)}(u) + \tilde{X}^{(3)}(u) + \tilde{X}^{(4)}(u) \tag{4.2b}$$

where

$$X^{(i)}(u) = \frac{Q^{(i-1)}(u-1)}{Q^{(i-1)}(u)}\,\frac{Q^{(i)}(u+1)}{Q^{(i)}(u)}\,f^{(i)}(u) \qquad \text{and}$$

$$\tilde{X}^{(i)}(u) = \frac{Q^{(i-1)}(u+i-2)}{Q^{(i-1)}(u+i-3)}\,\frac{Q^{(i)}(u+i-3)}{Q^{(i)}(u+i-2)}\,f^{(5-i)}(u).$$

We now choose $u = 0$, so that the $X^{(1)}$, $X^{(4)}$, $\tilde{X}^{(1)}$, $\tilde{X}^{(4)}$ vanish (this, once again, can be interpreted as a consequence of the requirement that two loops of the same colour do not cross each other). Finally, we consider the two-row matrix $\mathbf{T} = \mathbf{T}_{\square}\mathbf{T}_{\begin{smallmatrix}\square\\\square\end{smallmatrix}}$. Its eigenvalue is obtained by taking the product of the remaining terms in equations (4.2); rewriting the $X^{(i)}$ as functions of $Q^{(i)}$, getting rid of the extra factors $\sin\gamma$ which compensate the factors of c in equation (3.8), we find the eigenvalues of T to be

$$\begin{aligned} t &= 2\frac{Q^{(2)}(1)Q^{(2)}(-1)}{Q^{(2)}(0)^2} + \frac{\omega^{(2)}}{\omega^{(3)}}\left(\frac{Q^{(2)}(1)}{Q^{(2)}(0)}\right)^2 \frac{Q^{(1)}(-1)}{Q^{(1)}(0)}\,\frac{Q^{(3)}(0)}{Q^{(3)}(1)} \\ &\quad + \frac{\omega^{(3)}}{\omega^{(2)}}\left(\frac{Q^{(2)}(-1)}{Q^{(2)}(0)}\right)^2 \frac{Q^{(1)}(0)}{Q^{(1)}(-1)}\,\frac{Q^{(3)}(1)}{Q^{(3)}(0)} \\ &= \left(a^{-1}\frac{Q^{(2)}(1)}{Q^{(2)}(0)}\sqrt{\frac{Q^{(1)}(-1)}{Q^{(1)}(0)}\,\frac{Q^{(3)}(0)}{Q^{(3)}(1)}} + a\frac{Q^{(2)}(-1)}{Q^{(2)}(0)}\sqrt{\frac{Q^{(1)}(0)}{Q^{(1)}(-1)}\,\frac{Q^{(3)}(1)}{Q^{(3)}(0)}}\right)^2 \end{aligned} \tag{4.3}$$

where in the last line we have used the explicit expression of the twist. This is precisely the square of the expression found in [11] for the one-row transfer matrix. The notation is as follows:

$$u_k \equiv 2\mathrm{i}\big(u_k^{(1)} + 1/2\big) \qquad v_k \equiv 2\mathrm{i}\big(u_k^{(3)} - 1/2\big) \qquad w_k \equiv 2\mathrm{i}\, u_k^{(2)}. \tag{4.4}$$

Furthermore, the Cartan subalgebra produces three conserved quantities; in fundamental and conjugate representations, they have the following expression (basis of the dual of the root lattice):

$$\left.\begin{matrix} Q_{1\,\square} \\ -Q_{1\,\begin{smallmatrix}\square\\\square\end{smallmatrix}} \end{matrix}\right\} = \begin{pmatrix} 1&0&0&0\\0&0&0&0\\0&0&0&0\\0&0&0&0 \end{pmatrix} - \frac{1}{4}I \quad \cdots \quad \left.\begin{matrix} Q_{2\,\square} \\ -Q_{2\,\begin{smallmatrix}\square\\\square\end{smallmatrix}} \end{matrix}\right\} = \begin{pmatrix} 1&0&0&0\\0&1&0&0\\0&0&0&0\\0&0&0&0 \end{pmatrix} - \frac{1}{2}I \quad \cdots \quad \left.\begin{matrix} Q_{3\,\square} \\ -Q_{3\,\begin{smallmatrix}\square\\\square\end{smallmatrix}} \end{matrix}\right\}$$
$$= \begin{pmatrix} 1&0&0&0\\0&1&0&0\\0&0&1&0\\0&0&0&0 \end{pmatrix} - \frac{3}{4}I. \tag{4.5}$$

Combining this with the corresponding representation given in figure 3, it will be easier to identify them with the components of the charge Q of equation (2.3). Their value is determined by the numbers $m^{(i)}$ of Bethe roots of kind i: each root of kind i decreases by one the ith component of the charge, starting from the reference state which has $Q = \binom{L}{L}$. Comparing with equation (2.3), we deduce that

$$m^{(1)} = N_{w\downarrow} + N_{eb} \qquad m^{(2)} = N_{\downarrow} \qquad m^{(3)} = N_{w\downarrow} + N_{ob}. \tag{4.6}$$

Note that if $m^{(1)} > 0$ but $m^{(3)} = 0$, only even arrows are modified compared to the reference state (i.e., all odd arrows are white pointing up); and similarly for $m^{(3)} > 0$, $m^{(1)} = 0$ and odd arrows.

5. Results and conclusions

We have found that the nested algebraic Bethe ansatz can be used to solve the FPL^2 model at $n_b = n_w$. The latter is therefore identified with a standard integrable vertex model associated with $U_q(\widehat{sl(4)})$. Its weights, combined in 2×2 square blocks of vertices, satisfy a Yang–Baxter equation; its two-row transfer matrix is embedded into an infinite set of commuting transfer matrices; and many results follow immediately.

In particular, the long distance behaviour of this type of model has been studied by many methods (see for instance [18–21]). For $|n| > 2$, the spectrum has a gap and the correlation length is finite. In the following we focus instead on the critical regime $|n| \leqslant 2$, and we parametrize $n = 2\cos\gamma$.

As our model is isotropic, we expect the largest eigenvalue of the transfer matrix to have the following asymptotic behaviour [22]:

$$\log t_0(L) = -Lf_0 + \frac{\pi c}{6L} + \cdots \qquad \text{for} \quad L \to \infty \tag{5.1}$$

where c is the central charge of the infrared conformal field theory. Here, note that only fundamental representations ($\square$ and $\begin{smallmatrix}\square\\\square\end{smallmatrix}$) are used, so we deal with a non-fused model. Assuming the usual form for the ground state, standard computations (see, e.g., [21]) lead, in this type of model, to the following form of c:

$$c = r - \frac{3}{\pi(\pi-\gamma)}\,\langle w|\, C^{-1}\,|w\rangle \tag{5.2}$$

where r and C are, respectively, the rank and the Cartan matrix of the underlying algebra and w is a vector with components $w_s = \frac{1}{\mathrm{i}}\log(\omega^{(s)}/\omega^{(s+1)})$, that parametrizes the twist. If we now specialize to A_3 and to our choice of boundary conditions: $w_1 = w_3 = 0$, $w_2 = -2\gamma$, we obtain

$$c = 3 - 12\frac{\gamma^2}{\pi(\pi-\gamma)} \tag{5.3}$$

which coincides with what was found in [4]. Note that this is not the central charge of the $W(A_3)$ conformal field theory—the latter can also be obtained within the framework of this model, but with a different twist.

One can also investigate the nature of excitations above the ground state. They are, of course, gapless and describe solitons associated with the three fundamental representations of A_3 interacting with the standard S-matrices [21, 23], plus possible bound states in certain regimes of γ. In the infrared limit the dispersion relation can be linearized and the corresponding low-lying excited states are related to the conformal weights Δ_n of the aforementioned CFT via

$$\log t_n(L) = -Lf_0 + \frac{\pi(c-24\Delta_n)}{6L} + \cdots \qquad \text{for} \quad L \to \infty. \tag{5.4}$$

One can check that the weights thus obtained fit with the formulae of the Coulomb gas picture:

$$\Delta_n = \tfrac{1}{4}\langle e|\, K^{-1}\, |e-2e_0\rangle + \tfrac{1}{4}\langle m|\, K\, |m\rangle \tag{5.5}$$

where $K = \frac{1}{2}(1-\gamma/\pi)C$, e (resp. m) is the electric (resp. magnetic) charge which belongs to the lattices of weights (resp. roots) of A_3 and e_0 is the background charge related to our twist by $e_0 = \frac{1}{2\pi}w$. This constitutes a confirmation of the results of [5]. Incidentally, the fact that for $n_b \neq n_w$ the quadratic form K appearing in the conformal weights, as given in [5], is generically not related to a Cartan matrix can be considered an indication of the non-integrability of the model.

We have made some numerical checks of the structure of the ground state and excited state described above. It turned out that, this picture was confirmed for $n \geqslant 0$; however, for $n < 0$ the ground state of the usual form (with, using the notation of equation (4.4), real u_k, v_k, w_k) is *not* the state corresponding to the dominant eigenvalue of the transfer matrix. Indeed, we have found an $n \to -n$ symmetry of the eigenvalue spectrum corresponding to the sectors where both $L - m^{(2)}$ and $m^{(1)} + m^{(3)}$ are even, cf equation (4.6); this applies thus in particular to the ground-state sector which has $m^{(1)} = m^{(2)} = m^{(3)} = L$. This symmetry can be described in the Bethe ansatz equations as the transformation of the Bethe roots (with the notation of equation (4.4)):

$$\gamma u_k \to -(\pi-\gamma)u_k \qquad \gamma v_k \to -(\pi-\gamma)v_k \qquad \gamma w_k \to -(\pi-\gamma)w_k + \mathrm{i}\pi \tag{5.6}$$

where we recall that $n = 2\cos\gamma$, so that $-n = 2\cos(\pi-\gamma)$. One can check that this transformation leaves the eigenvalues (4.3) invariant. In particular, we conclude that the 'real' ground-state eigenvalue t_0 only depends on $|n|$ and identifies with the one described above only for $n \geqslant 0$. For $n < 0$, the 'fake' ground-state eigenvalue corresponds to a state very high above the real ground state (even the bulk part differs as $L \to \infty$ [11]), whose special property is that it is the analytic continuation of the $n > 0$ ground-state eigenvalue. For example, at $n = -2$, the (fake) ground-state eigenvalue found in [11] is equal to 2 irrespective of L, whereas the largest eigenvalue diverges exponentially with L.

Note that the situation where two levels corresponding to different free energies f_0 and to different finite-size corrections c, are present in the same transfer matrix is not unheard of. For example, the zero-temperature Ising antiferromagnet is equivalent to a one-component height

model, whose continuum limit is a free bosonic field, whence $c = 1$ [24]. On the other hand, the same model also resides on the self-dual curve of the q-state Potts model on which it is integrable; by specializing the results valid on that curve, one finds $c = -25/2$ and a different bulk free energy. There is no contradiction in this, since the amplitude of the latter eigenvalue vanishes at $q = 2$. It is possible that a similar phenomenon occurs in the FPL^2 model, at least for some discrete values of $n < 0$, but establishing this would require further investigations. In particular, proper care must be taken in specifying the boundary conditions and in treating winding loops.

We remark that the symmetry of the ground-state sector holds true more generally for the $n_b \neq n_w$ FPL^2 model, under the transformation $(n_b, n_w) \to (-n_b, -n_w)$. This is based on the observation that, with suitable periodic boundary conditions, all terms in the high-fugacity expansion of the partition function have $N_b + N_w$ even, where N_b (resp. N_w) is the number of black (resp. white) loops. To see this, represent the dominant state at $n_b, n_w \to \infty$ as an 'ideal state' in the four-colouring picture [1], with black (resp. white) loops being an alternation of colours 1 and 2 (resp. 3 and 4). Note that the high-fugacity expansion of the 1–2 (black) and 3–4 (white) loops (disregarding their orientation) can be obtained by only permuting the colours around the two *other* types of small loops (say, of types 1–3 and 2–4), and that these loops remain of length 4. Examining all possible 1–2 and 3–4 loop environments of a plaquette occupied by the 1–3 and 2–4 loops proves our statement.

It is interesting to compare our results with the work of Reshetikhin [25] on fully packed loops on the hexagonal lattice. After contracting the vertices of the hexagonal lattice two by two, so as to form a square lattice, this author identified the R-matrix with that of the integrable model $U_q(\widehat{sl(3)})$. The choice of spectral parameter, as in our case, makes $\check{\mathbf{R}}$ degenerate into a projection operator. However, there are important differences. First, in [25] the underlying algebra is of course different and all horizontal and vertical lines carry the same representation $\square$ of $U_q(\widehat{sl(3)})$, in contrast to the alternation of $\square$ and $\begin{smallmatrix}\square\\\square\end{smallmatrix}$ used here. Second, in [25] there is no twist Ω in the auxiliary space, whence contractible and non-contractible loops carry respective weights of n and 2. In particular, for $n \leqslant 2$, the central charge is constant, $c = 2$. When $n = 2$, the continuum limit of the hexagonal-lattice loop model becomes an $SU(3)_{k=1}$ free field Wess–Zumino–Witten theory; this is a consequence of the $U_q(\widehat{sl(3)})$ identification and of the fact that only the fundamental representation is used. Likewise, the $U_q(\widehat{sl(4)})$ identification of the FPL^2 model reported in the present work implies that the $n = 2$ case is an $SU(4)_{k=1}$ WZW theory in the continuum limit. Indeed, the four-colouring model was originally constructed by Read [2] so as to have an $SU(4)_{k=1}$ symmetry. It would be interesting to study the relation of integrable models based on $U_q(\widehat{sl(N)})$, with $N > 4$, to more general models of colourings and/or of fully packed loops.

References

[1] Kondev J and Henley C L 1995 Four-coloring model on the square lattice—a critical ground state *Phys. Rev.* B **52** 6628–39

[2] Read N 1992 *Proc. Kagomé Workshop* ed P Chandra (Princeton, NJ: NEC Laboratories)

[3] Raghavan R, Henley C L and Arouh S L 1997 New two-color dimer models with critical ground states *J. Stat. Phys.* **86** 517–50 (*Preprint* cond-mat/9606220)

[4] Kondev J 1997 Liouville field theory of fluctuating loops *Phys. Rev. Lett.* **78** 4320–3 (*Preprint* cond-mat/9703113)

[5] Kondev J and Jacobsen J L 1998 Conformational entropy of compact polymers *Phys. Rev. Lett.* **81** 2922–5 (*Preprint* cond-mat/9805178)

[6] Jacobsen J L and Kondev J 1998 Field theory of compact polymers on the square lattice *Nucl. Phys.* B **532** 635–88 (*Preprint* cond-mat/9804048)
[7] Jacobsen J L and Kondev J 2004 *Phys. Rev.* E **69** 066108
[8] Jacobsen J L and Kondev J 2004 *Phys. Rev. Lett.* **92** 210601
[9] Batchelor M T, Blöte H W J, Nienhuis B and Yang C M 1996 Critical behaviour of the fully packed loop model on the square lattice *J. Phys. A: Math. Gen.* **29** L399–404
[10] Nienhuis B 2001 Tiles and colors *J. Stat. Phys.* **102** 981–96 (*Preprint* cond-mat/0005274)
[11] Dei Cont D and Nienhuis B 2004 *J. Phys. A: Math. Gen.* **37** 3085–3100
[12] Reshetikhin N 1990 *Lett. Math. Phys.* **20** 331
[13] Foerster A, Links J and Roditi I 1998 Integrable multiparametric quantum spin chains *J. Phys. A: Math. Gen.* **31** 687–95 (*Preprint* cond-mat/9801175)
[14] Delius G W, Gould M D and Zhang Y-Z 1994 On the construction of trigonometric solutions of the Yang–Baxter equations *Nucl. Phys.* B **432** 377–403 (*Preprint* hep-th/9405030)
[15] Babelon O, de Vega H J and Viallet C-M 1982 *Nucl. Phys.* B **200** 266
[16] Kulish P P and Reshetikhin N Yu 1983 Diagonalisation of $GL(N)$ invariant transfer matrices and quantum N-wave system (Lee model) *J. Phys. A: Math. Gen.* **16** L591
[17] Bazhanov V V and Reshetikhin N Yu 1990 Restricted solid-on-solid models connected with simply laced algebras and conformal field theory *J. Phys. A: Math. Gen.* **23** 1477
[18] Pokrovski S and Tsvelik A 1987 *Sov. Phys.–JETP* **66** 1275
[19] de Vega H 1987 Finite-size corrections for nested Bethe ansatz models and conformal invariance *J. Phys. A: Math. Gen.* **20** 6023
de Vega H 1988 Integrable vertex models and extended conformal invariance *J. Phys. A: Math. Gen.* **21** L1089
[20] Zhou Y and Pearce P 1995 Solution of functional equations of restricted $A^{(1)}_{n-1}$ fused lattice models *Nucl. Phys.* B **446** 485–510
[21] Zinn-Justin P 1998 Non-linear integral equations for complex affine Toda associated to simply laced Lie algebras *J. Phys. A: Math. Gen.* **31** 6747 (*Preprint* hep-th/9712222)
[22] Blöte H W J, Cardy J L and Nightingale M P 1986 Conformal invariance, the central charge, and universal finite-size amplitudes at criticality *Phys. Rev. Lett.* **56** 742
Affleck I 1986 Universal term in the free energy at a critical point and the conformal anomaly *Phys. Rev. Lett.* **56** 746
[23] Hollowood T J 1993 *Int. J. Mod. Phys.* A **8** 947
[24] Nienhuis B, Hilhorst H J and Blöte H W J 1984 Triangular SOS models and cubic-crystal shapes *J. Phys. A: Math. Gen.* **17** 3559–82
[25] Reshetikhin N Y 1991 A new exactly solvable case of an $O(n)$ model on a hexagonal lattice *J. Phys. A: Math. Gen.* **24** 2387–96